Energetic particle shower in the vapor from electrolysis

R. A. Oriani*

University of Minnesota, Minneapolis, MN 55419

J. C. Fisher†

600 Arbol Verde, Carpinteria, CA 93013

(Dated: December 19, 2004)

Abstract

Approximately 40,000 energetic charged particles were recorded in a pair of plastic detector chips suspended in the vapor over an active electrolysis cell. Particle track locations and orientations were revealed by examining the etch pits produced by chemical etching. Analysis of track orientations indicates that the shower originated in a compact source in the vapor between the chips. The total magnitude of the shower is estimated to have been 150,000 particles and its duration is estimated to have been a few seconds. A previously unknown type of nuclear reaction is indicated.

*orian001@umn.edu

†fisherjc@earthlink.net

I. INTRODUCTION

For over a decade, beginning with Fleischmann and Pons [1], there have been claims of unusual experimental results suggesting room temperature nuclear reactions of a new kind. They include generation of excess energy above input energy during electrolysis, production of helium and tritium, generation of energetic charged particles, transmutation, and other essentially nuclear phenomena. The bibliographies prepared by Storms [2][3] provide overviews of this work. The nuclear claims have not been generally accepted by the physics community. Yet research in this area continues, directed to finding and demonstrating results of sufficient magnitude and clarity that skepticism can be overcome.

Because energetic charged particle phenomena are among the clearest indicators of nuclear processes, we have concentrated our efforts in this direction. Using CR-39 plastic detectors in electrolysis experiments we have observed particle tracks consistent with energetic alphas. Initially we immersed the detectors in the electrolyte [4][5]. We observed an excess of particle tracks over those in control chips similarly exposed without active electrolysis. Our results were variable with an overlap between the track densities observed for active chips and for control chips, but after many repetitions of the experiment statistical analysis showed a highly significant correlation between active electrolysis and energetic particle generation. Although these results were convincing to us they still left room for doubt by the larger community.

We next supported detector chips in the vapor above the electrolyte. In most experimental runs we obtained densities of tracks that exceeded the background of incidental radon tracks by an average factor of about three [6]. But in five runs we found the remarkable result of a factor of a hundred above background. One such shower originated in the vapor between a pair of chips and generated tens of thousands of recorded tracks. Describing and interpreting these tracks is the subject of this paper.

II. EXPERIMENTAL PROCEDURE

The experimental setup is identical with that employed in earlier experiments [4][5] except that the detector chips were suspended in the vapor above the electrolyte. The electrolysis cell is an open-ended vertical glass cylinder 10 cm long and 1.6 cm inside diameter with a

sheet of palladium clamped to the lower end and sealed by O-rings. The palladium serves as cathode. The upper end of the cell is partially closed by a stopper and the cell is partially filled with an electrolyte having an initial composition of 2.3 g Li_2SO_4 per 100 cc H_2O. A 2 mm diameter titanium rod supported by the stopper bears two pairs of 0.1 mm diameter hooks on which CR-39 detector chips are suspended. A platinum wire spot-welded to the rod ends in a horizontal pancake spiral that serves as the anode. A nickel disc that nearly fills the cross-section of the cell is supported by the rod above the surface of the electrolyte. It serves to mitigate carry-over of mist from the electrolyte to the detector chips suspended above it. It also blocks charged particles originating in the electrolyte from impinging upon the detector chips. In the experiment here described two pairs of chips were hung edge down, members of each pair being roughly parallel to each other and about 8 mm apart.

Electrolysis was conducted for three days during which time the detector chips were surrounded by $O_2 + H_2$ vapor. Energetic particles that entered the chips from the vapor produced latent tracks of internal damage along their trajectories. After electrolysis the chips were etched in 6.5N KOH for approximately 20 hours at 60C. The etching process attacks damaged material along latent tracks more rapidly than it attacks undamaaged material, generating pits that mark the intersections of particle tracks with the surface of the chip.

III. TRACK NUMBERS AND ORIENTATIONS

Here we analyze the pattern of tracks from a shower in the vapor between a pair of detector chips. We begin with the chip having the higher track density. After etching to develop latent tracks, the side that was exposed to the shower was photographed in a mosaic of 270 photographs. A representative photograph is reproduced in Fig. 1. From these photographs a montage of 1044 rectangular images (4:3 ratio of sides) was obtained by subdividing each photograph into four equal images and discarding those few images that extended beyond the edges of the chip. Etch pits were counted in each area where counting was possible. Counting was not possible where the chip had a hole for its support wire, had identification numerals laser-inscribed by the manufacturer, or in four images that had damage of unknown cause. Images that could not be completely counted were retained if more than half of the image was available. Their count numbers were adjusted upward assuming an equal density

for the missing part of the image as for the measured part. Overall about 90% of the chip surface was counted.

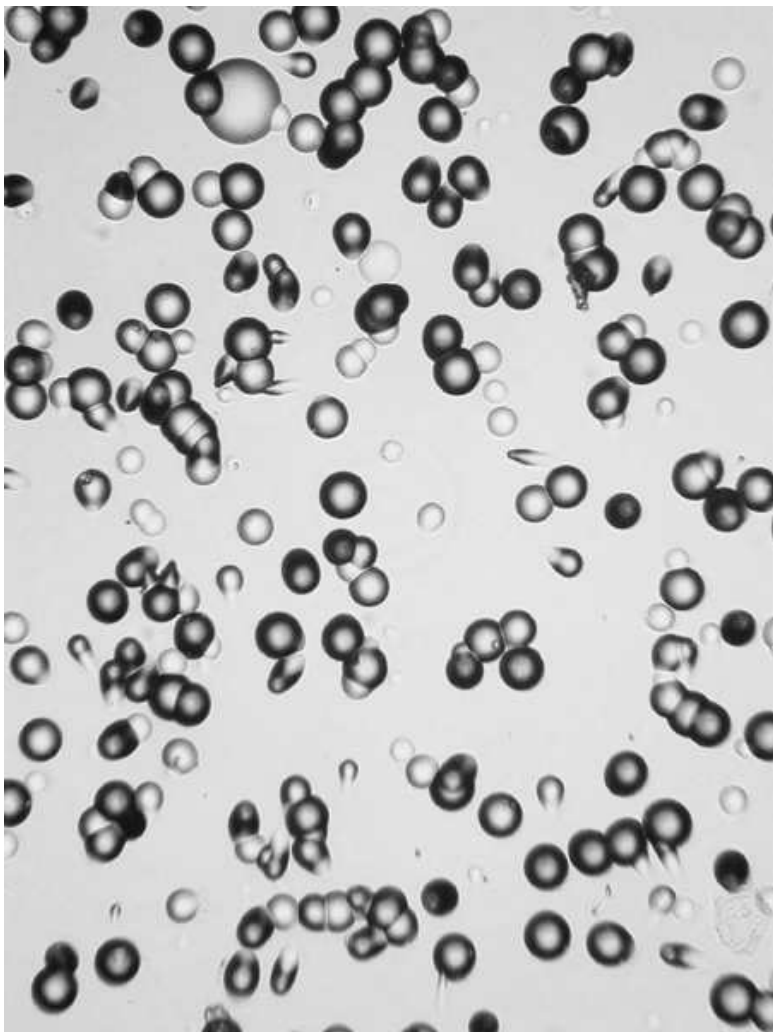

FIG. 1: Etch pits on the surface of a CR-39 plastic detector chip suspended in the vapor over an active electrolysis cell. Each pit marks the location of a track of damaged material where a charged particle has penetrated the chip. A roughly conical pit has developed during etching because the etchant attacks the damaged material of the track more rapidly than it attacks the adjacent undamaged material. The area shown measures approximately 0.29mm x 0.22mm. The mean diameters of the darker circular pits are approximately 24 microns.

We counted 29,800 etch pits in the portion of the chip available for counting, and estimate by interpolation that another 3,300 particles passed undetected into unavailable areas, giving a total of 33,100 charged particles impinging upon or passing through the 1044 images. By

analyzing the shadow cast by the support hook we estimate that an additional 240 particles were stopped by the wire and did not reach the detector chip. Adding these the final total is about 33,300 charged particles impinging on the area of 1044 images.

A smoothed contour plot of the density of etch pits is shown in Fig. 2A. The units are etch pits per image. (Because the area of an image is about $6.3(10)^{-4}$ cm^2 one must multiply by 1600 to obtain etch pits per cm^2.) The solid contour lines are spaced at 10 pits per image and range from 10 pits per image along the right side to a maximum of 110 pits per image near the lower left corner of the chip. From its maximum the density of pits falls to below 10 pits per image near the right side of the chip, reaching a level of 3 pits/image at the dashed contour line. This is the etch pit density we customarily find in chips exposed to the vapor in experiments where we do not see a massive shower such as the one under discussion. The dashed contour line thus marks a boundary beyond which no shower particles left tracks capable of producing pits upon etching. In addition to its prominent position along the right side of the chip this boundary comes close to the lower left corner of the chip. (The image at the lower left corner of the chip contains 10 pits. The 10 pits per image contour line should pass through it, although this is not shown in the figure because the contour algorithm requires more than a single data point to determine a contour segment. The gradient of pit density suggests that the 3 pits per image contour line then lies just beyond the corner of the chip.)

Also shown in Fig. 2A is an indication of the directions of the tracks near the perimeter of the densely pitted area. Track orientations can be determined from the shapes of the etch pits as described more fully below. Eight areas were selected around the perimeter and one near the center of the chip, each consisting of four contiguous images. Within each such area the orientations were determined for those etch pits for which a clear measurement was possible. Where necessary the microscope was focused at several levels from the surface into the interior of the plastic to aid the determination. Each pit with a measured orientation was assigned a unit vector in the direction of the track as seen in its projection on the surface of the chip. These vectors were added to obtain the mean track direction, and the cosine of the angle between each constituent vector and the mean track orientation was determined. The mean cosine provides a measure of the extent to which the vectors are aligned. When the mean cosine is near unity the constituent vectors must be nearly parallel. When the mean is near zero the constituent vectors must tend to point equally in opposite directions.

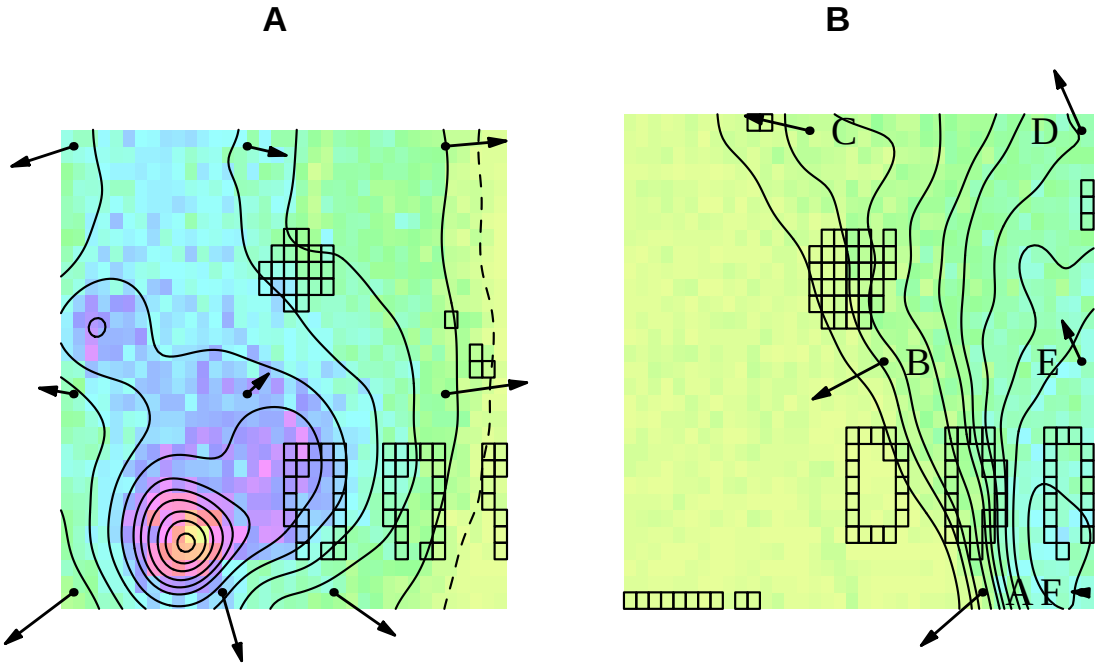

FIG. 2: Distribution of etch pits on the surfaces of CR-39 plastic detector chips suspended in the vapor over an active electrolysis cell. **(A)** The more heavily pitted chip. Density in pits/image is indicated by the color scale for a mosaic of 1044 images that span the approximately 8mm square surface. Outlined images could not be counted and etch pit densities were interpolated for them; those in the upper portion of the chip correspond to the support hole and those in the lower portion correspond to laser-inscribed identification numbers. The solid contour lines are spaced at 10 pits/image and range from 10 pits/image along the right side to 110 pits/image near the peak. The dashed contour line denotes 3 pits/image. Arrows indicate mean orientations of tracks having elliptical etch pits. Arrow lengths are proportional to the mean cosines of the angles between individual track projections on the surface of the chip and the corresponding arrow orientation. **(B)** The facing chip at a distance of about 8mm. A 2mm supporting rod ran vertically between the detectors. The smoothed contour lines are spaced at 3 pits/image and range from 3 pits/image on the left to 30 pits/image at the peak. The area of low etch pit density over much of the detector lies in the shadow of the supporting rod. It indicates that the shower originated in a small volume close to and nearly behind the support rod. The edge of the shadow is not parallel to the edge of the detector chip, suggesting that the chip was canted with respect to the rod or that the active volume moved sideways as it rose.

The arrows in Fig. 2 indicate the mean orientation of the tracks in each area, and their lengths are proportional to the mean cosines of the track projections along these directions. Clockwise beginning at the lower left corner the mean cosines and (in parentheses) the numbers of tracks from which they were determined, are 0.956(35), 0.387(43), 0.726(30), 0.453(49), 0.686(20), 0.925(30), 0.838(20), 0.798(72); and for the central arrow they are 0.331(58).

We see that in the lower left corner of the chip, and along the lower contour lines on the right side, the tracks are strongly aligned pointing away from the central region of high track density. On other parts of the perimeter the tracks also tend to align pointing away from the central region but with more scatter as indicated by the smaller values of mean cosine. It is clear that the tracks originated somewhere in the vapor above the densely pitted surface of the chip. But they cannot have arisen from a stationary source because the extended region of high track density does not have rotational symmetry.

Working back from the boundary determined by the dashed contour line, we can obtain a rough idea of the height of the particle source above the surface of the chip. During etching a roughly conical pit develops because the etchant attacks the damaged material of the track more rapidly than undamaged material. Etching causes the vertex of the cone to move into the plastic more rapidly than it causes the surface to recede. The vertex points in the direction that the energetic charged particle traveled as it entered the plastic. The axis of the cone coincides with the track of travel and the shape of the etch pit depends on the orientation of the axis and on the half-angle of the cone. When the axis is nearly perpendicular to the surface the intersection of the etch pit with the surface is nearly circular. It becomes increasingly elliptical as the orientation of the axis tilts away from the perpendicular.

Now consider the etching process when the damage trail makes only a small angle with the surface of the chip. Consider a spot on the damage trail inside the chip. This spot lies closer to the surface than to the beginning of the damage trail where the particle entered the plastic. As the etching process proceeds the surface of the chip etches toward the spot at a steady rate. Etching proceeds along the damage trail at a faster rate but it has farther to go. At a critical angle, equal to the half-angle of the cone, the surface and the apex of the cone reach the spot at the same time. For damage trails with angles smaller than the critical value relative to the surface of the chip the surface gets there first and no etch pits can form.

All shower particles must have been generated near enough to the chip that none of them left an etchable track beyond the dashed boundary in Fig. 2A. This implies that beyond the boundary none of them made an angle as large as the cone half-angle with the chip surface. Measurement and analysis of cone angles indicates a half-angle of about 19 degrees as described below, so we can deduce that all particles were generated below a sloping surface that rises from the boundary at a slant angle of 19 degrees in the direction opposed to the arrows in the lower left corner and along the right side of the chip. The tent-like roof suggested by these rafters reaches a height of about 1mm from the chip surface in the neighborhood of the peak, indicating that the source of energetic particle generation did not extend above this level. It reaches a height of about 3mm near the upper edge of the chip suggesting that the particle source moved away from the chip or grew in diameter as it progressed upward toward and past the support hole. We envision an active volume having an initial diameter of a fraction of a millimeter that began emitting particles in the vapor about 1 mm from the chip near its lower left corner, just touching the tent-like roof, then moved upward along the chip in a wandering path occasionally touching and defining other portions of the roof along the way.

Because the densely populated area extends beyond the dimensions of the chip in some directions, only a rough estimate can be made of the total number of charged particles generated in the shower. We estimate that about 50,000 etch pits would have been counted had the chip been sufficiently extended, and considering that tracks making angles less than 19 degrees with the surface do not produce etch pits we estimate about 150,000 charged particles as the total number in the full 4π steradians of the shower.

The second chip is slightly larger than the first. It was photographed in a mosaic of 285 photographs, from which a montage of 1140 images was obtained by quartering each photograph. Following the same procedure as with the first chip we found that a total of about 10,700 charged particles left etch pits in the detector chip or passed undetected into areas unavailable for counting. A contour plot of the density of etch pits for the second chip is shown in Fig. 2B. A portion of the chip exhibits a maximum in track density roughly opposed to the peak density in Fig. 2A. In this area the variation of track density with position mirrors that in Fig. 2A with track density values that are about one-third as great. The rest of the chip shows a very low level of track density, comparable with the background level in Fig. 2A, that we interpret as lying in the shadow of the 2mm rod from which the

chips were suspended. It appears from the orientation of the boundary of the shadowed region that the chip was hung in a canted orientation with respect to the support rod, or perhaps that the active volume moved sideways as it rose between the detector chips.

Because the shower originated in the vapor above a relatively warm electrolyte we expect convection currents that would carry away the vapor near a chip in a matter of seconds. The fact that we observe a somewhat confined and well-defined volume in which the particles originated suggests that the duration of the major part of the shower did not exceed a few seconds.

The arrows in Figs. 2A and 2B provide aggregate measures of the orientations of particle tracks in selected small target areas. Each aggregate includes tracks that produced elliptical etch pits for which track orientations could be determined. Tracks having nearly circular pits, for which no orientations could be established, were necessarily omitted. If we consider a target area directly under a distant source, such that a perpendicular from the source to the plane of the target lies within the target, tracks formed in the target can make only small angles with the perpendicular. The more distant the source the smaller the angles will be and the more nearly circular the etch pits will be. Depending on the size of the source, its distance from the target area, and the ability of microscopic examination to detect small differences from circularity, it can turn out that no orientations at all can be established in a target area directly under the source. In this event orientations can be determined only if the target area lies off to one side of the source.

Fig. 3 summarizes individual orientations for the six target areas indicated by arrows in Fig. 2B. Tracks in target areas A, B, and C on the left side of the heavily pitted portion of the chip point to the left, away from the heavily pitted area, indicating that the responsible particles came from the direction of the heavily pitted area to their right. For these target areas track orientations were obtainable for an average 62% of all etch pits. The patterns of tracks are quite different in the three targets on the right side of the chip, for which orientations were obtainable for only 27% of etch pits. Tracks in target area F in the lower right are confined to a pair of narrow angular spreads pointing upward and downward. The upward-pointing tracks correspond to a source below the target and the downward-pointing tracks correspond to a source above the target. We interpret these tracks as originating in a compact source that moved upward in the vapor approximately 7mm distant from the chip at the beginning of its trajectory. Before the source reached a position above the target area

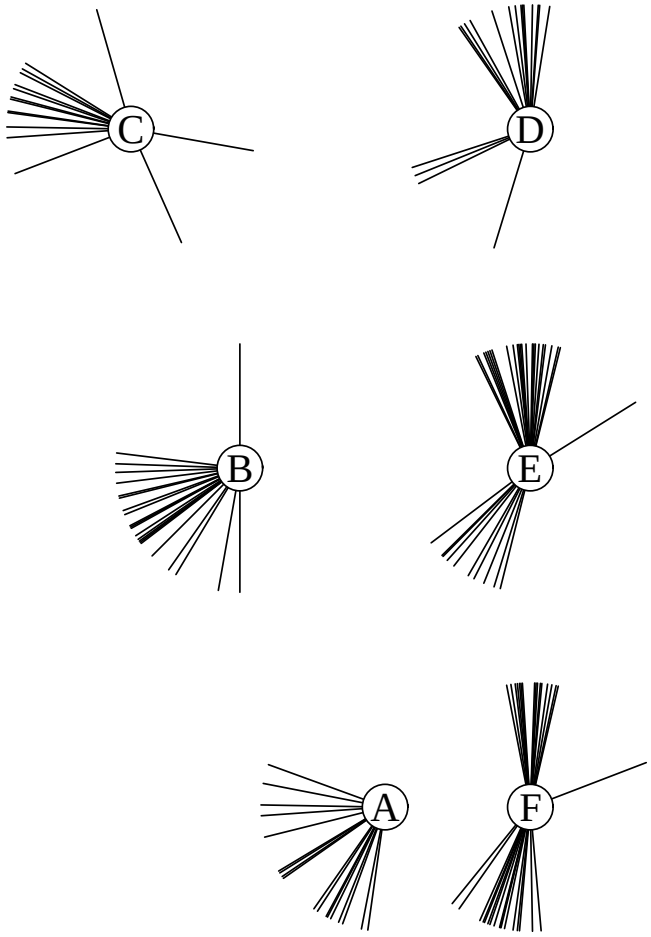

FIG. 3: Individual orientations for tracks that produced elliptical etch pits in target areas A–F in Fig. 2B. As described in the text the pattern of tracks in areas D–F indicates that a compact source of energetic particles drifted in the vapor in the general direction from F toward D, passing over and progressively to the right of these target areas.

the tracks were directed ahead of it in the upward direction. After it had passed the target the tracks were oriented behind it in the downward direction. When the source was directly overhead all tracks were nearly perpendicular to the target, the etch pits were nearly circular and their orientations could not be determined.

The track orientations in target area E indicate that the compact source passed nearly over this area as well, but slightly to the right beyond the edge of the chip. The orientations in target area D suggest that the source continued its motion along more or less the same trajectory. In each of the images D, E, and F where there is a clear division into two distinct spreads of orientations, the upward-pointing tracks were generated earlier than the

downward-pointing ones. Because the activity of the source had a short lifetime, we expect the number of upward-pointing tracks in each target to exceed the number of downward-pointing ones, reflecting a decline of activity between the times at which the leading and following tracks were formed. The data are consistent with this expectation, recognizing that the compact source first became active near location F leading to a shortfall of upward-pointing tracks at that location from what would be expected had the source become active farther away.

The patterns seen in Fig. 3 have counterparts in the data from Fig. 2A, but because the compact source was much closer to the first chip than to the second, the angle subtended by the source as seen from a target area in Fig. 2A was large enough that particles originating from the perimeter of the source produced oriented tracks at a location even when the center of the source was directly over that location. These tracks from a nearby overhead source add clutter to the record of a moving source that otherwise is so clearly evident in Fig. 3 for a more distant source.

IV. PARTICLE TRACK ANALYSIS

Etch pits arise from various causes. Some result from alpha particles from decay of radon in the air or from superficial damage to the plastic detector and others from the energetic particle tracks that are the subjects of this analysis. Track pits initially are conical in shape with the vertex located on the track and the axis of the cone aligned with the track. The conical shape arises because damaged material along a track etches away more rapidly than the surrounding undamaged material. At first the depth and diameter of a pit increase proportionately as etching proceeds, but when the end of the track is reached the etching rate in the track direction slows to that of undamaged material and the point of the cone rounds out. The pit has "bottomed out". The portion of the pit near the surface of the plastic continues for a time to retain its conical shape and its diameter grows at an unchanging rate. Then as the surface of the plastic etches away to the depth of the end of the track the pit completely loses its conical shape and it progressively approaches the shape of a nearly circular dish. Pits from superficial damage bottom out very soon because the damage extends only a short distance into the plastic. They become shallow circular dishes shortly after etching begins.

Examination of tracks produced by radon from a pitchblende source indicates that the track lengths for radon alphas are only slightly longer than the depth of plastic that is removed by the etching process. Tracks that are nearly perpendicular to the surface of the detector produce sharp-pointed pits, but tracks that make a modest angle with the perpendicular bottom out because the surface etches down past their far ends. Bottoming out is particularly pronounced when tracks from radon alphas are etched a second time. After the second etch all pits are circular or nearly circular dishes with diameters nearly twice that of single-etched tracks. One such pit is visible at the top of Fig. 1.

In order to eliminate background events and to distinguish between families of etch pits, we employ various combinations of the following data restrictions. Let R be the ratio of the major axis to the minor axis of a pit. By imposing the restriction $R \geq 1.1$ to remove circular and nearly circular pits we can eliminate most of the pits that arose from sites of superficial damage, and also the pits that were formed in the initial etch and then were etched again after electrolysis. By imposing the restriction $R \leq 1.5$ we retain only those pits whose geometric mean diameter is a good approximation to the diameter of a circular pit of the same energy impinging normal to the chip surface. By imposing a restriction to include only those etch pits that are observed under the microscope to be sharp-pointed cones we retain only pits that have not bottomed out. And conversely by imposing a restriction to exclude pits with sharp-pointed conical shape we retain only pits that have bottomed out. In the following analysis we always apply the restrictions $1.1 \leq R \leq 1.5$ and we sometimes additionally apply restrictions relating to the presence or absence of sharp-pointed conical pits.

We expect that some of the tracks recorded in the shower chips were caused by alpha particles from decay of radon in the laboratory environment. The magnitude of such contamination was explored in a number of control runs in which detector chips were suspended in the vapor over the electrolyte in the absence of electrolysis [6]. The chips were etched to reveal pre-existing tracks, and then they were photographed in tagged areas that could be identified later, were mounted in the inactive cell, exposed for three days, removed, etched and photographed again to reveal the tracks associated with influences of the laboratory environment during the initial photography, mounting, exposure, and etching procedures. The densities of etch pits from tracks formed during these procedures amounted on average to 150 ± 70 pits/cm^2.

In searching for tracks from radon contamination of the shower chips we first photographed, counted, and determined the shapes and mean diameters of all etch pits on the back side of the primary shower chip in Figure 2A. The back side was shielded by the chip itself from the shower on the front side. The mean etch pit diameters are shown in Fig. 4A. Before applying the restrictions $1.1 \leq R \leq 1.5$ to remove nearly circular and strongly elliptical pits the peak near 17 μm contained about 160 pits/cm^2. This density lies within the range of control densities previously noted. Hence we conclude that the 17 μm pits indicate tracks from radon in the laboratory environment during photography before electrolysis and that they provide a standard for pits on the shower sides of both chips.

Measurements of etch pit dimensions on the shower sides of the chips give quite different results. First we examine the etch pits on the second shower chip in the shadow of the support rod which covers half the area of the chip. Here we expect alphas from radon decay as observed on the back side of the primary shower chip, and possibly other particles from decay of a few long-lived products of the shower reaction that may have drifted to where their decay products could reach the shadow region. Fig. 4B shows the size distribution of these etch pits in the shadow region. Two peaks are evident, one near 17 μm corresponding to the peak in Fig. 4A and a new peak with larger etch pits near 24 μm having no counterpart in Fig. 4A. Microscopic examination shows that the larger etch pits have bottomed out near the end of the etching process, but to a lesser extent than the pits that result from double etching of radon alphas. We can analyze the two peaks by considering the three-dimensional shapes of the pits. In Fig. 5 we retain only those pits that are observed not to have bottomed out. Specifically they must have the shapes of sharp-pointed cones. This restriction removes the family of larger etch pits, and the remaining distributions (Figs. 5A, 5B) for sharp-pointed conical pits are statistically indistinguishable. Both clearly reflect contamination by alpha particles from radon decay.

Next we turn attention to the family of larger etch pits that have just begun to bottom out. In Fig. 6 we plot distributions of pit sizes where now we retain only those pits that are observed to have bottomed out (*i.e.* they must not have the shapes of sharp-pointed cones). Fig. 6A shows the distribution for pits on the shaded area of the chip in Fig. 2B, and Fig. 6B shows the distribution for pits on the front surface of the primary shower chip in Fig. 2A. These distributions are statistically indistinguishable, strongly suggesting that the family of larger etch pits identifies tracks of charged particles emitted from precursors whose lifetimes

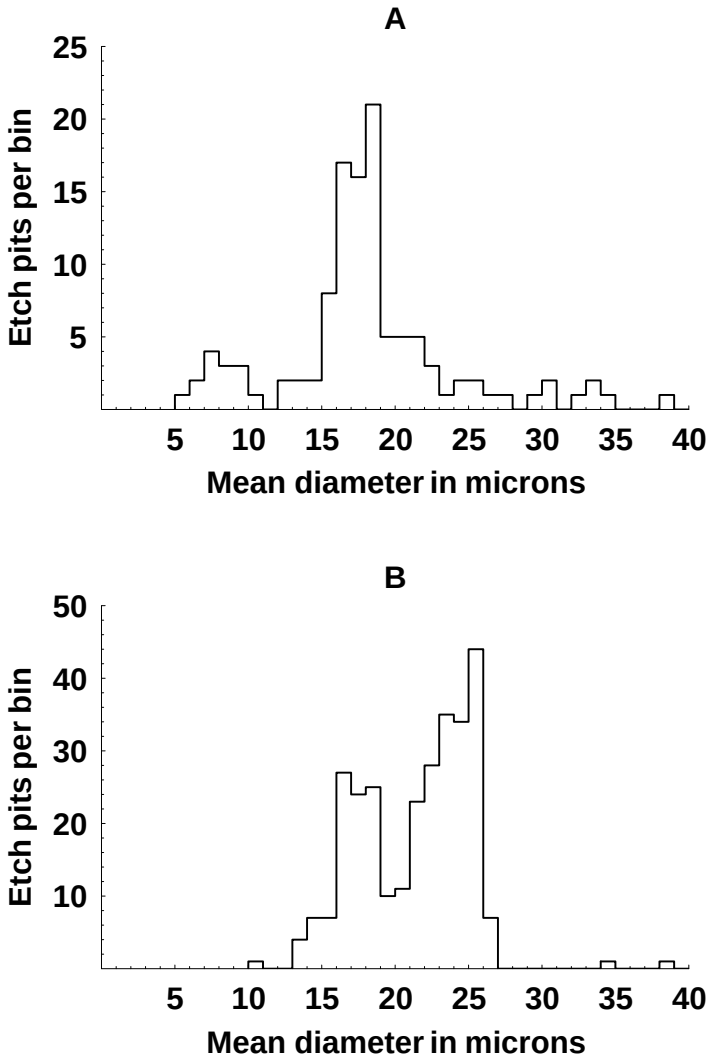

FIG. 4: Etch pit sizes (geometric means of maximum and minimum pit diameters) on two chip surfaces. **(A)** Back side of the chip in Fig. 2A, shielded by the chip itself from the particle shower on the front side. **(B)** Shaded area of the front side of the chip in Fig. 2B, shielded from prompt shower particles by the support rod. These plots include all etch pits with ratios of maximum to minimum diameters in the range $1.1 \leq R \leq 1.5$. The restriction $1.1 \leq R$ eliminates the circular and nearly circular pits from pre-existing tracks. The restriction $R \leq 1.5$ eliminates highly elliptical pits for which the geometric mean diameter ceases to be a good approximation to the diameter for normal track incidence.

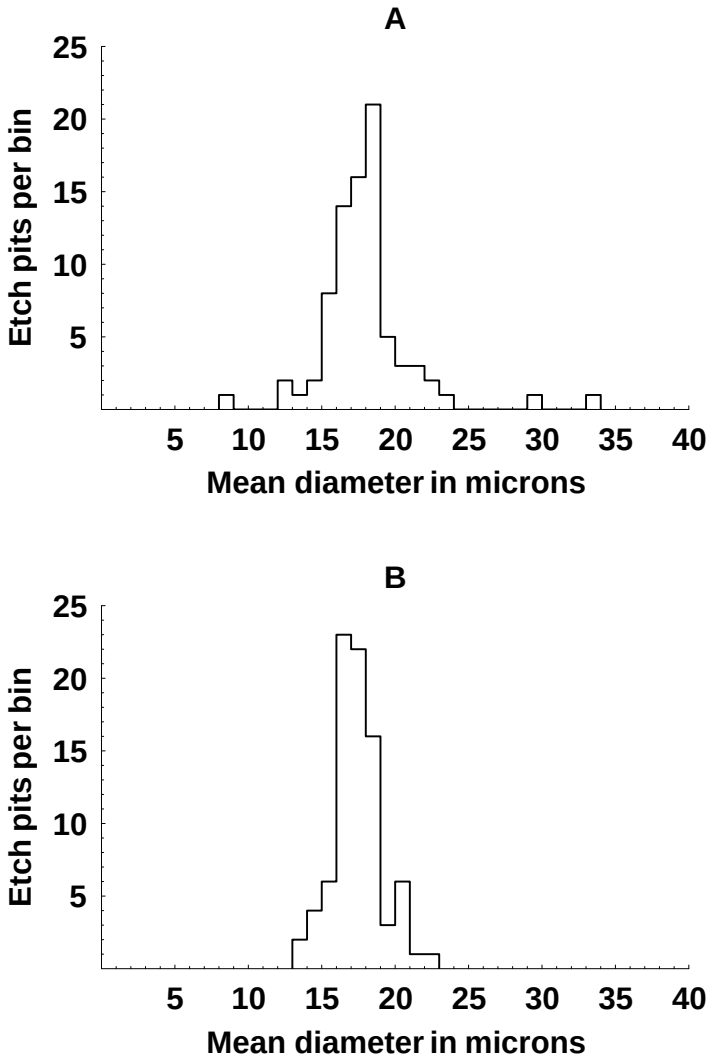

FIG. 5: Etch pit sizes on the two chip surfaces of Fig. 4. Subject to the data cut $1.1 \leq R \leq 1.5$ as in that figure and additionally restricted to include only sharp-pointed conical pits that have not bottomed out. **(A)** Back side of the primary shower chip in Fig. 2A. **(B)** Shadowed area on the front side of the secondary shower chip in Fig. 2B.

are sufficiently long that a few have drifted into the region between the support rod and the shadowed area of the second shower chip.

We now can confirm the 19° value of the half-angle of the shower pits whose trajectories bounded the location of the shower source. From Fig. 5 the mean diameter of the radon alpha tracks in the peaks of the distributions is 17.4 ± 1.0 μm. From Fig. 6 the mean diameter of the new tracks in the peaks of their distributions is 24.1 ± 1.2 μm. Comparing the diameter

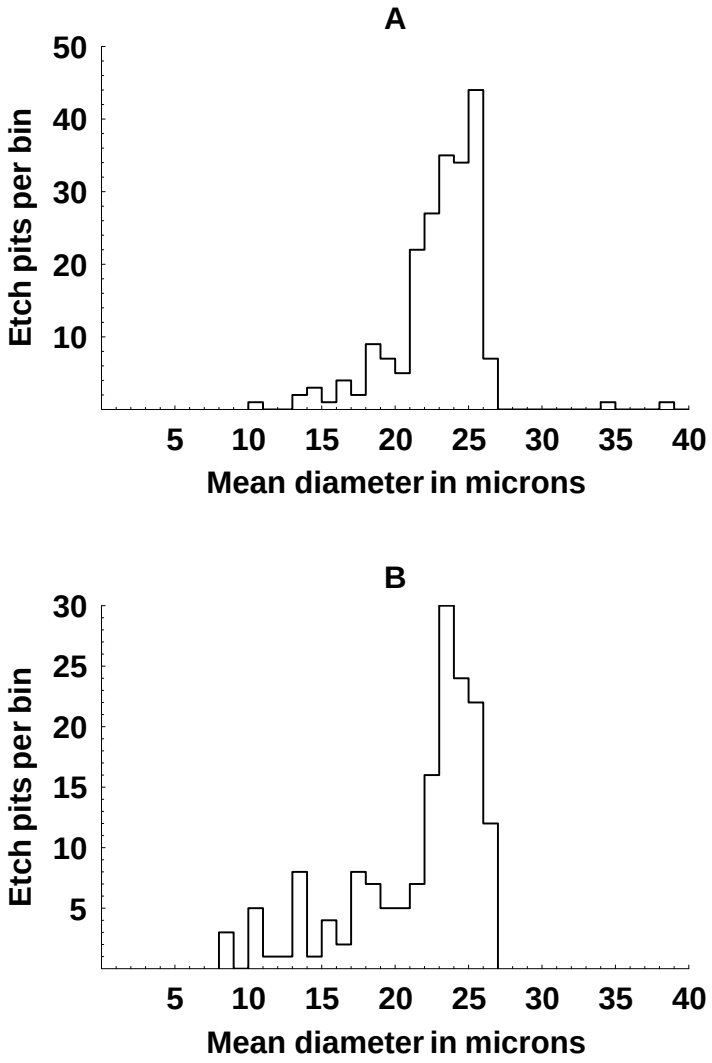

FIG. 6: Etch pit sizes on two chip surfaces subject to the cuts $1.1 \leq R \leq 1.5$ and additionally restricted to exclude sharp-pointed conical pits. The remaining pits have bottomed out. **(A)** Shadowed area on the front side of the secondary shower chip in Fig. 2B. **(B)** Sample of the front surface of the primary shower chip in Fig. 2A.

of the new tracks to that of radon alpha tracks the ratio is $(24.1\pm1.2)/(17.4\pm1.0) = 1.4\pm0.1$. Analysis of the etching process leads to a relationship between the half-angle θ of a conical etch pit, the pit diameter D at the surface of the detector chip, and the depth of etching S of the flat surface, $D/S = 2(1 - \sin\theta)/\cos\theta$. Sharp-pointed conical pits from radon alphas occasionally are found on surfaces perpendicular to the detector chip such as the edges of the chip and the edges of laser-inscribed numerals. The side views of these pits

facilitate measurement of cone angles, and suggest a half-angle $\theta = 36^{\rm o}$ for radon alphas. Substituting this value of θ in the equation gives $(D/S)_{\rm radon} = 1.02$. Because the new alphas have diameter 1.4 times as great we have $(D/S)_{\rm new} = 1.43$ corresponding to $\theta = 19^{\rm o}$.

Particle identities and energies can be determined using methods described by Fleischer, Price, and Walker[7]. We first consider the relationship between etch pit half-angle and particle energy for protons and the corresponding relationship for alpha particles. Quantitative relationships for CR-39 plastic were provided by Fleischer[8]. The shower particles cannot be protons because there is no energy for which protons produce tracks with 19^o half-angles. For alpha particles the energy corresponding to a $19^{\rm o}$ half-angle is 2.0 MeV, suggesting that the shower particles could be alphas.

Energies also can be deduced from measurements of etch pit diameters. Roussetski *et al.* [9], in support of their research on the emission of charged particles in various systems, have determined etch pit sizes for alphas having a wide range of accurately known energies. Their calibration curve for diameter D corresponding to energy E is well fit by the relationship $D^{3.5}E$ = constant over the energy range $1.85 \leq E \leq 7.19$ MeV. From this relationship we have $E_2/E_1 = (D_1/D_2)^{3.5}$. With $D_2/D_1 = 1.4 \pm 0.1$ this gives $E_2/E_1 = 0.31 \pm 0.04$ for shower particles interpreted as alphas relative to radon alphas. Radon decays to stable ^{210}Pb in a cascade of reactions including three that generate alpha particles: $^{222}{\rm Rn} \longrightarrow {}^{218}{\rm Po} + \alpha$, $^{218}{\rm Po} \longrightarrow {}^{214}{\rm Pb} + \alpha$, and $^{214}{\rm Po} \longrightarrow {}^{210}{\rm Pb} + \alpha$. These alphas have energies 5.5 MeV, 6.0 MeV, and 7.8 MeV respectively and are expected with equal frequency. Taking the mean value $E_1 = 6.4$MeV we find that the energy of the shower particles would be $E_2 = (0.31 \pm 0.04)(6.4) = 2.0 \pm 0.3$ MeV if they were alphas. This confirms the determination from half-angle analysis. It is unlikely that nuclei with higher charge and mass would have sufficient range in the vapor to reach the detector chips and form etchable tracks, and hence in view of the available evidence we tentatively identfy the shower as 2 MeV alpha particles.

V. CONCLUSIONS

Our observations furnish compelling evidence for a nuclear process that generated a shower of charged particles in an oxygen-hydrogen vapor. It appears to have consisted of a rapid reaction that generated a cloud of unstable intermediate particles whose decay products were the observed shower particles, tentatively identified as 2 MeV alpha particles.

We can think of no explanation for this phenomenon in terms of conventional nuclear theory, and believe that an extension of the theory is required.

Acknowledgments

We thank M. E. Fisher for assistance in data presentation.

---

[1] M. Fleischmann, S. Pons, M. Hawkins: J. Electroanal. Chem. **261**, 301 (1989) and **263**, 187 (1989).

[2] E. K. Storms: J. Sci. Exploration **10**, No.2, 186 (1996)
(full text in `http://www.scientificexploration.org/jse/articles/storms/1.html`).

[3] E. K. Storms: *Infinite Energy* **4**, No. 21, 16 (1998)
(full text in `http://pw1.netcom.com/~storms2/review5.html`).

[4] R. A. Oriani, J. C. Fisher: Jpn. J. Appl. Phys. **41**, 6180 (2003) and **42**, 1498 (2003).

[5] R. A. Oriani, J. C. Fisher: Trans. Am. Nuc. Soc. **88**, 640 (2003).

[6] R. A. Oriani, J. C. Fisher: Proc. 10th Int. Conf. Cold Fusion, 2003.

[7] R. L. Fleischer, P. B. Price, R. M. Walker, Nuclear Tracks in Solids, University of California Press, Berkeley, CA (1975).

[8] R. L. Fleischer, private communication.

[9] A. S. Roussetski, A. G. Lipson, V. P. Andreanov: Proc. 10th Int. Conf. Cold Fusion, 2003.